NIH Public Access
Author Manuscript
*Mol Pharm*. Author manuscript; available in PMC 2013 November 05.

Published in final edited form as:
*Mol Pharm*. 2012 November 5; 9(11): 3089–3098. doi:10.1021/mp300221f.

# The Interactions between L-Tyrosine Based Nanoparticles Decorated with Folic Acid and Cervical Cancer Cells Under Physiological Flow

**Andrew J. Ditto**[a,b], **Kush N. Shah**[a,d], **Nikki K. Robishaw**[c], **Matthew J. Panzner**[c], **Wiley J. Youngs**[c], and **Yang H. Yun**[a,*]

[a]Department of Biomedical Engineering, The University of Akron, Olson Research Center, Akron, OH 44325-0302, USA

[b]Department of Biochemistry and Cancer Biology, University of Toledo, Health Sciences Campus, Toledo, OH 43614, USA

[c]Department of Chemistry, The University of Akron, Knight Chemical Laboratory, Akron, OH 44325-3601, USA

[d]Department of Integrated Bioscience, The University of Akron, Auburn Science and Engineering Center, Akron, OH 44325-3908, USA

## Abstract

Many anticancer drugs have been established clinically, but their efficacy can be compromised by nonspecific toxicity and an inability to reach the desired cancerous intracellular spaces. In order to address these issues, researchers have explored the use of folic acid as a targeted moiety to increase specificity of chemotherapeutic drugs. To expand upon such research, we have conjugated folic acid to functionalized poly(ethylene glycol) and subsequently decorated the surface of L-tyrosine polyphosphate (LTP) nanoparticles. These nanoparticles possess the appropriate size (100–500 nm) for internalization as shown by scanning electron microscopy and dynamic light scattering. Under simulated physiological flow, LTP nanoparticles decorated with folic acid (targeted nanoparticles) show a 10-fold greater attachment to HeLa, a cervical cancer cell line, compared to control nanoparticles and to human dermal fibroblasts. The attachment of these targeted nanoparticles progresses at a linear rate, and the strength of this nanoparticle attachment is shown to withstand shear stresses of 3.0 dynes/cm$^2$. These interactions of the targeted nanoparticles to HeLa are likely a result of a receptor-ligand binding, as a competition study with free folic acid inhibits the nanoparticle attachment. Finally, the targeted nanoparticles encapsulated with a silver based drug show increased efficacy in comparison to non-decorated (plain) nanoparticles and drug alone against HeLa cells. Thus, targeted nanoparticles are a promising delivery platform for developing anticancer therapies that over-express the folate receptors (FRs).

### Keywords

Nanoparticles; Biodegradable polymer; Targeting; Folate receptors; Cancer

*Corresponding Author: Dr. Yang H. Yun, Department of Biomedical Engineering, University of Akron, 301 Buchtel Common, Akron, OH, 44325-0302, Tel: 330-972-6619, yy@uakron.edu.

**Supporting Information**

Results include an MP4 file of targeted nanoparticles attaching to HeLa at shear stress of 0.5 dyne/cm$^2$, which can be viewed with QuickTime movie player, and a table for the cumulative release of SCC22 from LTP nanoparticles. This material is available free of charge *via* the Internet at http://pubs.acs.org.

$watermark-text
$watermark-text
$watermark-text

$watermark-text

$watermark-text

$watermark-text

## INTRODUCTION

Targeting tissues with high specificity is a challenge for a variety of therapeutics.[1–3] This issue is especially critical for the delivery of chemotherapeutic agents since the drug's toxicity is usually detrimental to the overall health of the patients.[4, 5] To add specificity, researchers have examined a variety of receptor binding molecules[6] including antibodies[7] and peptides.[8] Despite promising pre-clinical studies, the synthesis and purification of peptides are typically slow, and laborious, [9] and antibodies can have stability issues during chemical conjugation and when exposed to the biological fluids.[10] As a result, small molecular weight targeting molecules, such as vitamin B12,[11] bombesin,[12] and folic acid[13, 14] have been an intense area of research. Previous studies have shown the potential targeting abilities of folic acid due to the over-expression of the FRs in cancer cells found in breast, brain, and cervix; myeloid cells;[15] and activated macrophages.[13, 14] Ovarian carcinomas are especially attractive targets since they express FRs at consistently high levels as compared to normal tissues.[16–18]

FRs exist in three isoforms of which the FR-α has high affinity and the ability to transport folic acid into cells.[16, 19] In general, tumors over-expressing the FR-α are better suited as candidates for using folic acid as targeting moieties.[16] Once these molecules binds to FRs, they are endocytosed, released, and the receptors are cycled back to the cell surface to be used again within 30 minutes.[20] If the folic acid is directly conjugated to the drugs using covalent bonds, such as thioether conjugation, the drug may not be able to cleave from the complex. These complexes have decreased potency by over four orders of magnitude when compared to the drug alone.[21] Furthermore, the therapeutic efficacy of most conjugated drugs directly to folic acid can be limited by loading capacity and the lack of solubility of common solvents. These results demonstrate the necessity of a cleavable linker between the folic acid and the conjugated drug, or a targetable delivery system that releases the drug itself, such as biodegradable nanoparticles. Additional advantages of using biodegradable nanoparticles include high loading capacity of therapeutic drugs, encapsulation of multiple drugs including hydrophilic and hydrophobic compounds, enhanced drug stability, the release the drug over an extended time period, and the ease of surface decoration for targeting.

A biodegradable nanoparticles formulated with LTP, a 'pseudo' poly(amino acid) with a molecular weight of 8 to 10 kDa,[22–24] could be an ideal polymer for targeted therapy. LTP degrades within the lifetime of most cells [23]. The degradation products of LTP have been shown to be nontoxic and to have a negligible effect on local pH and non-cytotoxic.[22, 23] The plain nanoparticles already have demonstrated cellular uptake and a weeklong drug release in primary human dermal fibroblasts *in vitro*.[22, 25] Despite the ability to be internalized,[22] the LTP nanoparticles have yet to be decorated with a targeting moiety.

We have decorated the surface of LTP nanoparticles by blending copolymer of polyethylene glycol and polylactic-co-glycolic acid conjugated to folic acid (PLGA-PEG-Fol) into the double emulsion formulation of the nanoparticles, which would thermodynamically favor the accumulation of targeting molecules at the water-oil interface. While previous *in vitro* studies have examined the cancer targeting abilities of polymeric nanoparticles decorated with folic acid,[26–29] few of these researchers have investigated the receptor-ligand interactions under simulated physiological flow conditions. Tumors are known to have a leaky vasculature; thus, targeted nanoparticle of appropriate size could transition from capillary fluid flow (ranging from 0.5 to 8 dynes/cm$^2$)[30] to shear stress as low as 0.05 dynes/cm$^2$.[31] The changes in the hemodynamic forces as the nanoparticles exit the microvascular network could influence the binding of the nanoparticles and the receptor-ligand

$watermark-text

$watermark-text

$watermark-text

interactions. Therefore, this study will characterize the adhesion properties of LTP nanoparticle decorated with folic acid against HeLa cells under fluid flow that simulates conditions within capillaries. Since hemodynamic forces influence the transport and attachment of nanoparticles, we will quantify number of nanoparticle attachment, the binding kinetics, and the strength of folic acid and FR interactions.

## EXPERIMENTAL SECTION

### Visualization of Folate Receptors

The expression of FRs was visualized with immunofluorescence assay. HeLa-S5 cells (HeLa, ATCC, Manassas, VA) were seeded into a 24 well tissue culture plate at a density of 25,000 cells per well in 0.5 mL of feeding media (44% Dulbecco's Modified Eagle Medium, 44% Nutrient Mixture F-12, 10% new born calf serum, 1% antibiotic/antimycotic, 1% GlutaMAX, and 4.5 mg/mL glucose). The following day, cells were fixed with 1% formaldehyde, and the nonspecific sites of antibody (Ab) interactions were blocked with 1% calf serum (Hyclone, Rockford, IL) for 30 minutes and washed with PBS. The application of monoclonal anti-FR IgG (1:100 dilution, Enzo Life Sciences, Plymouth Meeting, PA) lasted overnight at 4°C [32]. The cells were then washed with PBS, blocked again with serum, and applied with goat anti-mouse IgG conjugated to TRITC (1:1000 dilution, Sigma-Aldrich, St. Louis, MO) for one hour. The immunostaining samples were imaged using a microscope (Axiovert 200, Carl Zeiss, Peabody, MA), a CCD camera (AxioCam HRm, Carl Zeiss, Peabody, MA), and Axiovision 4.7 software (Carl Zeiss, Peabody, MA). The exposure settings for the camera and the post process for the experimental and control images were identically set and handled, respectively. Primary human dermal fibroblasts (passage 6–8, a gift from Judy Fulton at the Kenneth Calhoun Research Center, Akron General Medical Center, Akron, OH) were used as a non-cancerous control.

### Conjugation of Folic Acid to PEG-PLGA

PLGA-PEG-Folate was synthesized according to the protocol established by Yoo and Park.[33] Briefly, PLGA (MW of 4200 Daltons, Evonik Industries, Essen, Germany) was activated with dicyclocarbodiimide (DCC) and N-hydroxy succinimide (NHS) using a stoichiometric mole ratio of 1:2:2 for PLGA:DCC:NHS, respectively. This reaction was performed under a nitrogen blanket and using methylene chloride as a solvent. The product of the reaction was precipitated with chilled diethyl ether, and dried to constant weight under vacuum. The activated PLGA was then reacted to PEG-bis-amine (MW of 3400 Daltons, Laysan Bio, Arab, AL) at a stoichiometric mole ratio of 1:5 for the synthesis of PLGA:PEG–bis-amine using methylene chloride and under a nitrogen blanket. The resulting co-polymer was precipitated in chilled ether, filtered, and dried. Conjugation of folic acid to PLGA–PEG-amine was carried out in presence of DCC using dimethyl sulfoxide as a solvent. The final reaction was precipitated with water, unreacted impurities precipitated and removed by centrifugation, and the supernatant dialyzed and dried.

### Formulation of Targeted Nanoparticles

Targeted nanoparticles were formulated by blending LTP, copolymer of poly(lactic-co-glycolic acid) (PLGA-PEG), folic acid conjugated to PEG-PLGA (PLGA-PEG- Fol), and linear polyethylenimine (LPEI) and using a double emulsion of w/o/w and solvent evaporation technique. The typical targeted nanoparticle formulation consisted of an initial water-in-oil emulsion of 300 mg of LTP, 2.5 mg of PLGA-PEG, and 0.5 mg of PLGA-PEG-Fol dissolved in 3.0 mL of chloroform and 3 mg of LPEI in 1 mL of autoclaved distilled-deionized water ($DH_2O$, 1 mL) in a double neck 250 mL round bottom flask. To prepare nanoparticles with project average diameter of 2000 nm, the initial water-in-oil emulsion was vortexed for 1 minute at 2,000 RPM by impeller (Yamato Lab-Stirrer LR400D, Santa

$watermark-text

$watermark-text

$watermark-text

Clara, CA). The second water-in-oil-in-water emulsion contained 100 mL of 10% PVP and 10 mg/mL $NaNO_3$ added to the initial emulsion and vortexed for 3 minutes at 1,600 RPM. Chloroform was allowed to evaporate for 5 hours while being stirred and vented. Nanoparticles were collected and washed with $DH_2O$ by centrifugation at 12,000 × g for 20 minutes. Finally, nanoparticles were shell frozen in 10 mL of $DH_2O$, and placed in a lyophilizer (Labconco Freezone 4.5, Kansas City, MO) for 72 hours. The lyophilized nanoparticles were stored in desiccators.

Control (plain) nanoparticles were produced by the above procedure with the exception that the emulsion contained 3.0 mg of PLGA-PEG and lacked PLGA-PEG-Fol. For drug-loaded targeted nanoparticles, either 3 mg of cisplatin or 30 mg of silver carbene complex (SCC22)[34] was incorporated into the initial emulsion. SCC22 has been chosen for this study because of the resistance of HeLa to this drug.[34] FITC-labeled nanoparticles were prepared by the addition of 3 mg of FITC-BSA (Invitrogen, Carlsbad, CA) in the inner water phase. To prepare nanoparticles with an average projected diameter size of 200 nm, the same formulation was used except the initial emulsion was sonicated at 50% amplitude (Branson 102C CE, Danbury, CT) for 30 seconds. This initial emulsion was added to a secondary emulsion containing 10% PVP and vortexed for 3 minutes at 2,400 RPM.

### Scanning Electron Microscopy of LTP Nanoparticles Decorated with Folic Acid

Scanning electron microscopy (SEM, Hitachi S2150, Krefeld, Germany) was used to qualitatively visualize the size, shape, and morphology of all nanoparticle formulations. The SEM samples were prepared by suspending 1 mg of nanoparticles in 1 mL of $DH_2O$. Then, 200 OL of the suspended nanoparticles were pipetted onto a stub, dehydrated, sputter coated with silver/palladium and examined.

### Dynamic Light Scattering of LTP Nanoparticles Decorated with Folic Acid

Dynamic light scattering (DLS, Brookhaven Instruments BI-200SM, Holtsville, NY) was used to quantify size distribution of targeted nanoparticles. The nanoparticle sample was prepared by suspending 1 mg of nanoparticles in 10 ml of phosphate buffered saline (PBS, pH 7.4) that had been passed through a 0.2 μm filter. The suspended nanoparticles were centrifuged for ten seconds at 1000×g to remove any large aggregates. Then, the sample was decanted into a glass scintillation vial. The DLS system calculated the nanoparticle diameter by the Regularized Non-negatively Constrained Least Squares (CONTIN) method. The range of nanoparticle size was reported as differential distribution values, the results varied from 0 to 100, and reported as relative amounts.

### Attachment to Cancer Cells

An attachment study was performed based upon established methods[35, 36] to determine the interactions between the targeting system of targeted nanoparticles and HeLa cells. Twenty-four hours prior to the study, a 35 mm tissue culture dish (BD Biosciences, Bedford, MA) was coated with 1 ml of 5.5 μg/ml fibronectin (Invitrogen, Carlsbad, CA) and incubated for 30 minutes at room temperature. The fibronectin was removed and HeLa cells were seeded onto the plate at a density of 50,000 cells per plate in 2 ml of media. The cells were incubated overnight until a monolayer was formed. The cell media was removed and a parallel flow chamber (Glycotech, Rockville, MD) with a 0.254 mm gasket was placed on the cells. The procedure for the parallel flow chamber was followed according to the manufacturer's instruction.[37] This flow chamber set up was mounted onto a microscope and connected to a syringe pump (SP210IW Syringe Pump, World Precision Instruments, Sarasota, FL). Then, 1 mg of targeted or plain nanoparticles was suspended in 10 ml of 0.5% bovine serum albumin (BSA, Invitrogen, Carlsbad, CA) solution in PBS (pH 7.4). These suspended nanoparticles were drawn through the flow chamber and over the monolayer of

$watermark-text

$watermark-text

$watermark-text

cells at a shear stress of 0.5 dynes/cm$^2$ for 30 minutes. Afterwards, 5 ml of 0.5% BSA was drawn over the cells at a shear stress of 0.5 dynes/cm$^2$ to wash off any non-adherent nanoparticles. The attached nanoparticles were documented by recording 20 random fields with a CCD camera. The number of attached nanoparticles was quantified, and the attachment was reported as number of nanoparticles per mm$^2$. The attachment experiment was repeated using primary human dermal fibroblasts as a non-cancer control.

### Strength of Attachment of Nanoparticles Decorated with Folic Acid

The strength of the attachment between the targeted nanoparticles and the HeLa cells was determined by systematically increasing the shear stress. HeLa, fibroblasts, and targeted nanoparticles were prepared as described in the attachment study. Afterward, targeted nanoparticles perfused over the cells and allowed to rest on top of the cells for 5 minutes. Non-adherent nanoparticles were washed off. The attached nanoparticles were located, imaged, and quantified with microscopy. Next, the shear stress was increased from 0.5 dynes/cm$^2$ in increments of 0.25 dynes/cm$^2$ every 1 minute until the nanoparticles became detached. The detaching shear stress was recorded. This detachment was repeated for 10 nanoparticles per trial.

### Kinetics of Attachment for Nanoparticles Decorated with Folic Acid

The kinetics of the attachment between the targeted nanoparticles and the cancer cells were determined by visualizing the amount of attachment at various time intervals. HeLa, fibroblasts, and targeted nanoparticles were prepared as described in the attachment study. In this study, the flow was stopped at 2, 5, 10, and 15 minutes. At each time point, the nanoparticles attached were imaged and quantified. The imaging was repeated for 5 random locations per trial, and the rate of attachment was determined.

### Inhibition of Folic Acid Receptors

To confirm the receptor-mediated interaction for the targeted nanoparticles, a competitive assay was employed by the addition of folic acid dihydrate (Sigma Aldrich, St. Louis, MO) in the perfusion media. The concentration of 0.5, 1.0 and 2.0 mM was investigated, and the attachment study with free folic acid was repeated. If this molecule is in excess, the receptors should be blocked and unavailable for the LTP-PEG-Fol nanoparticle binding.[38]

### Anticancer Efficacy of Targeted Nanoparticles

The anticancer efficacy of targeted nanoparticles loaded with anticancer drugs, cisplatin and silver-carbene complex 22 (SCC22),[34] was examined under static conditions. HeLa cells were plated at a density of 25,000 cells/well and cultured as previously described. The following day, the cell culture media was replaced with media containing suspended nanoparticles (targeted and loaded with cisplatin, targeted and loaded with SCC22, plain and loaded with cisplatin, and plain and loaded with SCC22). The number of nanoparticles corresponded to the free drug exposed to cells (12 μM for SCC22 and 0.625 μM for cisplatin). After 30 minutes of incubation at 37°C, the cells were washed five times with PBS to remove any non-attached nanoparticles, given fresh media, and incubated for 3 days at 37°C. Afterwards, a LIVE/DEAD® cell assay was performed according to the manufacturer's instructions. Cytotoxicity was quantified using fluorescent microscopy. Fibroblasts were used as control cells. Additional controls were 500 μl of media, blank LTP nanoparticles, SCC22, and cisplatin.

### Statistical Analysis

The experimental methods were performed in triplicate. All quantitative data was tested for normality using the Shapiro-Wilk test. If the data was found to be normal, statistical

differences was determined using ANOVA analysis along with Tukey's post-hoc test. In the event that the data was not normal, a Kruskal Wallis one-way variance test was performed. The results were considered significant when $p \leq 0.05$.

## RESULTS

### Immunofluorescence of Folic Acid Receptors

An immunofluorescence assay of HeLa reveals elevated expression of FRs (Figure 1A). In contrast, fibroblasts show no detectable signs of FRs with this technique (Figure 1B). The HeLa's abundance of FRs suggests a potential mechanistic receptor mediated attachment of targeted nanoparticles to the cells.

### Shape and Size of Targeted Nanoparticles

Scanning electron microscopy shows the morphology of the targeted nanoparticles and they appear spherical in shape and smooth (Figure 2). When compared to previous formulations of the LTP nanoparticles (projected average diameter of 2000 nm), the surface decoration of folic acid does not change their morphology or shape.[22, 39] Dynamic light scattering shows diameter range between 1000 to 3000 nm with a mean of 1692 ± 188 nm (Figure 3A). For the nanoparticles with projected average diameter of 200 nm, the initial emulsion has been sonicated and the external water phase is mixed at high speed. These targeted nanoparticles have diameters ranging from 90 to 900 nm with a mean of 269 ± 131 nm (Figure 3B).

### Attachment of Nanoparticles Decorated with Folic Acid to Cancer Cells

The attachment study using a parallel flow chamber demonstrates the ability of targeted nanoparticles to attach to a monolayer HeLa under simulated physiological flow conditions. The average number of targeted nanoparticles attached to HeLa is 128 ± 8 nanoparticles per $mm^2$ (Figure 4). In contrast, the plain nanoparticle has a dearth of attachment at 21 ± 2 nanoparticles per $mm^2$, and the results are comparable attachment of targeted nanoparticles for non-cancerous fibroblasts at 22 ± 2 nanoparticles per $mm^2$ ($p > 0.999$). The differences in the attachment are also visible for the targeted and plain nanoparticles encapsulated with FITC (Figure 5). Thus, the attachment for targeted nanoparticles for HeLa is an order of magnitude higher than the control nanoparticles (Figures 4, $p < 0.001$). These attachment studies successfully demonstrate receptor mediated targeting of nanoparticles under simulated physiological flow (see supplementary data to observe a movie of targeted nanoparticle attachment to HeLa).

### Kinetics of Attachment for Nanoparticles Decorated with Folic Acid

The quantification of targeted nanoparticles to HeLa at various time points during their attachment establishes the kinetics of attachment. The targeted nanoparticles demonstrate a linear increase in attachment ($R^2 = 0.985$) over the course of their flow across HeLa (Figure 6). Imaged locations after the 20 minutes of attachment show increased numbers of nanoparticles as compared to after 15, 10, 5, and 2 minutes. After 10 minutes of perfusion, 62% ± 3% of the nanoparticle attachment has occurred, which is near half of the nanoparticles. This kinetics study exhibits that the attachment of targeted nanoparticles accumulates over time without any detectable detachment at 0.5 dynes/$cm^2$.

### Strength of Attachment for Nanoparticles Decorated with Folic Acid

The attachment strength of the targeted nanoparticles is determined by increasing shear stresses of 0.5% serum flow over attached nanoparticles to HeLa. The strength of the attachment is represented as the percentage of nanoparticles remaining at various shear stresses. These shear stresses range from 0.5 to 5.5 dynes/$cm^2$ at 0.25 dyn/$cm^2$ increments,



$watermark-text $watermark-text $watermark-text

$watermark-text

$watermark-text

$watermark-text

which begins to shear off cells from the plate as well (Figure 7). Until approximately 3.0 dynes/cm$^2$, nearly 90% of the nanoparticles remain attached, yet the results are not significantly different ($p = 0.999$) as compared to 0.5 dynes/cm$^2$. A significant decrease in nanoparticle attachment occurs at 4.9 dynes/cm$^2$ ($p = 0.008$), in which the percentage of nanoparticles remaining attached drops from 78% to 58%. At the highest shear stress of 5.5 dynes/cm$^2$, approximately 48% of the nanoparticles remain attached, which demonstrates a strong attachment comparable to the strength of HeLa's attachment to the fibronectin-coated plate.

### Inhibition of Folic Acid Receptors

In order to further determine whether the targeted nanoparticles are attaching to HeLa cervical cancer cells primarily by way of FRs, an inhibition study with excess folic acid in the perfusion solution is performed. Attachment is inhibited significantly ($p < 0.001$) at various concentrations of excess folic acid (Figure 8). The addition of 0.5 mM folic acid in the perfusion media decreases the number of LTP-Fol nanoparticles from 128 ± 8 to 30 ± 1 nanoparticles/mm$^2$. This inhibition is increased with 1.0 mM of folic acid in the 0.5% serum, which inhibits the attachment to 15 ± 1 nanoparticles/mm$^2$. A 2.0 mM concentration of folic acid further inhibits the attachment down to 12 ± 1 nanoparticle/mm$^2$. The targeted nanoparticle attachment to HeLa with both 1.0 mM and 2.0 mM of folic acid in the 0.5% serum is not significantly different ($p > 0.999$) than the plain LTP nanoparticles or the interactions of targeted nanoparticles to fibroblasts. This successful inhibition of attachment with excess folic acid is strong evidence that the targeted nanoparticles are attaching to the HeLa's FRs.

### Anticancer Efficacy of Folic Acid Decorated Nanoparticles

In order to determine the anticancer efficacy of the targeted nanoparticles, a monolayer of HeLa is incubated with the nanoparticles (encapsulated with SCC22 or cisplatin) or the drug for 30 minutes. The targeted LTP nanoparticles loaded with SCC22 or cisplatin have a significantly higher toxicity against HeLa as compared to plain LTP nanoparticles or the free drug ($p = 0.004$ and $p = 0.006$, respectively, Table 1). HeLa incubated with SCC22-LTP-Fol nanoparticles results in $LD_{50}$ of 12.0 μM of SCC22 (viability of 54 ± 10%), while plain SCC22-LTP nanoparticles result in a significantly higher viability of 93 ± 1%. The application of cisplatin-LTP-Fol nanoparticles against HeLa has resulted in a $LD_{50}$ of 0.625 μM. This result is significantly different to the free drug but not the plain nanoparticles loaded with cisplatin ($p < 0.001$ and $p = 0.207$, respectively). Hence, targeted nanoparticles in this study only significantly enhance the toxicity for the silver based chemotherapeutic drug. Finally, targeted nanoparticles loaded with SCC22 have little efficacy against fibroblasts (Table 1) with cellular viability of greater than 92% for all conditions while the toxicity of cisplatin loaded targeted nanoparticles resulted in viability of 64 ± 6%.

## DISCUSSION

The ligand-receptor interactions of folic acid conjugated to a therapeutic viable drug-delivery system has been characterized for the first time under physiological flowing conditions simulating conditions within capillaries. While many drug delivery system could have been chosen, LTP nanoparticles have shown promise as drug carriers for antimicrobials[40] and genes.[25] The modification for decorating the surface of LTP nanoparticles can be achieved by simply substituting the amphiphilic copolymers (2.5 mg of PLGA-PEG and 0.5 mg of PLGA-PEG-Fol instead of 3 mg of Chitosan-PEG) in the emulsion.[22, 24] While functionalized PEG groups could be chemically coupled to an assortment of molecules,[41, 42] we have focused upon FRs since they are overexpressed in ovarian, breast, brain, liver, and lung carcinomas.[42, 43] The overexpression of the FRs is also

$watermark-text

$watermark-text

$watermark-text

seen with HeLa (Figure 1A), and the targeted nanoparticles show 10 times greater binding efficacy as compared to plain nanoparticles ($p < 0.002$). A competitive assay confirms the ligand-receptor interaction of our targeted nanoparticles. The addition of free folic acid in the perfusion media, as expected, inhibits the attachment of the targeted nanoparticles (Figure 8). Notably, the attachment to HeLa with 1.0 mM folic acid is similar to the binding results for the plain nanoparticles against HeLa and fibroblast control experiments (Figure 4).

If the targeted nanoparticles are to be internalized along with the FRs, they must posses the appropriate size range for cellular uptake. Studies have shown that endocytosis of similar nanoparticles into cancerous cells is only possible if they are less than 4 μm in diameter.[44, 45] The uptake of the nanoparticles and their escape from endosomes are essential for most anticancer drugs, which require intracellular interactions.[46] Previous studies have documented that LTP nanoparticles can escape from endosomes and release DNA in the cytoplasm due to the proton sponge effect created by LPEI, which has been incorporated by design in the nanoparticle's formulation.[25, 47] Furthermore, the diameter of nanoparticles for cancer applications should be less than 200 nm, so they can take advantage of the enhanced permeability and retention effect and accumulate in the intercellular spaces.[48] The desired sizes of the targeted nanoparticles have been formulated (Figure 3B), but only the larger sizes are used to quantify the attachment and binding kinetics due to the limits of visualization with optics, flow chambers, and most CCD cameras. Although the influence of nanoparticle's diameter and their adhesion under flow has generally been established, an insight from a previous study shows that this relationship is independent of each other at low shear stresses under parallel flowing conditions.[35] To validate the binding kinetics for nanoparticles of less than 1000 nm, future studies will focus upon the mathematical modeling developed by Lauffenburger [49], which has been validated by experimentation.[35]

An obvious route for the administration of targeted nanoparticles is intravenous, which requires the nanoparticles to attach to cancer cells in the microcirculation.[50, 51] Thus, a high number of nanoparticle attachments at low shear stress is advantageous. When compared to previous studies with polystyrene (1 dyne/cm$^2$),[35] poly(e-caprolactone) (0.3 dynes/cm$^2$),[52] and hyaluronan (1 dynes/cm$^2$)[36] nanoparticles decorated with antibodies for E- and P-selectin show attachments ranging from 20 to 80 particles/mm$^2$ for Chinese Hamster Ovary cells that have been genetically modified to overexpress P-selectin. Thus, the use of folic acid to target cervical carcinoma is very attractive since the binding is greater than 120 nanoparticles/mm$^2$ (Figure 4), and the kinetics of attachment show a linear rate of accumulation (Figure 6). The targeted nanoparticles once bound and internalized, the FRs become temporarily unavailable, and they recycle back to the surface after releasing the ligand.[20] The rate of recycling is typically 30 minutes for HeLa.[20] After 20 minutes of perfusion, the binding kinetics show a linear relationship ($R^2 = 0.985$) and does not reach saturation. Thus, the FRs may always be available for nanoparticle binding and uptake.

In addition to the chemical interactions, the adhesion of targeted nanoparticles to the desired tumor is influenced by the fluid dynamics of the circulatory system and the interstitial space. Since tumor vascular is leaky, nanoparticles entering into the interstitial space from the microcirculation will be subject to a reduction of hemodynamic forces and will experience a shear stress gradient that could decrease as low as 0.05 dynes/cm$^2$.[31] Thus, the attachment of targeted nanoparticles to cervical carcinoma as well as the microcirculation of the tumor is possible for the range of shear stresses investigated. For larger arteries, the shear stress ranges from 10 to 70 dynes/cm$^2$.[53] As seen in Figure 7, the strength of attachment for targeted LTP nanoparticles is nearly steady between 0.5 to 3.0 dynes/cm$^2$, and nearly half nanoparticles are physically removed from the receptors when the shear stress reaches 5.0

$watermark-text

$watermark-text

$watermark-text

dynes/cm$^2$. This dependence on shear stress can act as a safety mechanism by preventing nonspecific adhesion of the targeted nanoparticles outside of the arteriole and capillaries regions.

The administration of chemotherapeutic drugs without a proper delivery system can fail to achieve effective killing of cancer cells due to their poor stability in physiological solutions,[54] rapid clearance from the tumor tissue,[55] inability of uptake,[56] and/or nonspecific toxicity.[57] Encapsulation of anticancer drugs into nanoparticles can overcome these issues and help with the localization within a carcinoma. Yet, encapsulation alone does not entirely prevent nonspecific toxicity or increase the uptake of drugs.[57] The decoration of the nanoparticle's surface with a targeting ligand is needed for preferentially binding as well as stimulating the uptake. The conjugation of folic acid to liposomes has shown increased drug internalization,[58] and this strategy should have the same effect for biodegradable nanoparticles. Although the internalization rate can vary among cancer cell types and the status of their metabolic cycles,[20] cervical cancer cells, such as HeLa, typically possess FR recycling rates of around half an hour.[20]

We have utilized the recycling rate of FRs by a 30 minute incubation of HeLa with targeted nanoparticles loaded with SCC22 or cisplatin followed by aggressive washing steps to remove non-adherent nanoparticles. Previous studies with SCCs have shown effectiveness against OVCAR-3 (ovarian, $LD_{50}$ ranging from 20 to 35 μM) and MB157 (breast 8 to 20 μM) cells lines, but HeLa has been shown to be resistant ($LD_{50}$ > 200 μM).[34] The characterization of viable cells after three days of incubation demonstrates a significant killing advantage of SCC22 encapsulated into targeted nanoparticles over the non-decorated nanoparticles and the drug alone (Table 1). Although the incubation time only lasted 30 minutes as opposed to 3 days in the previous published study,[34] the short incubation appears to be adequate for nanoparticles to bind with the FRs and for uptake by the HeLa cells. A $LD_{50}$ of approximately 12.0 and 0.625 μM (SCC22 and cisplatin, respectively) has been achieved with thorough washing steps to remove majority of non-adherent targeted nanoparticles (Table 1). For SCC22 loaded nanoparticles, the advantages of using folic acid as a targeting moiety can be clearly observed. Since the potency of SCC22 is much weaker than cisplatin ($L_{50}$ of > 200 μM verses ~ 3 μM, respectively, for the free drug with continuous incubation for 3 days), the advantages of encapsulation into targeted nanoparticles may only be gained for less effective drugs, such as carboplatin.[59, 60] The enhanced transport of cisplatin through non-specific endocytosis of drug loaded nanoparticles may be enough to kill both HeLa and fibroblast cells *in vitro* regardless of the specificity of targeting. However, this hypothesis will need to be tested in future research. In addition, human dermal fibroblasts exposed to targeted nanoparticles encapsulated with SCC22 have significantly lower toxicity ($p > 0.999$) as compared to HeLa. Therefore, the encapsulation of SCC22 into targeted nanoparticles appears to significantly increase its killing efficacy even in a cell line that is resistant to this drug. Finally, encapsulation of both chemotherapeutic drugs into nanoparticles, whether targeted or not, shows enhanced efficacy than the drug alone.

This investigation describes for the first time the binding characteristics of LTP nanoparticles decorated with folic acid in order to form a receptor mediated targeting drug delivery system. The decoration of the targeting group is accomplished with the incorporation of PLGA-PEG-Fol into the nanoparticles' emulsion during the formulation process. The targeted nanoparticles possess the necessary size for cancer drug delivery and receptor-based cellular uptake. These folic acid decorated nanoparticles are shown to bind to HeLa under simulated physiological flow conditions. Inhibition of this binding with excess folic acid demonstrates the likely binding of targeted nanoparticles to FRs on the HeLa. This study examines the mechanics of this binding by measuring the binding strength under

various shear stresses and the kinetics of the nanoparticle attachment. Finally, we show increased efficacy of drug delivery when incorporated into our targeted nanoparticles as compared to plain nanoparticles and drug alone. Altogether, the decoration of LTP nanoparticles with folic acid demonstrates their potential therapeutic values as a drug delivery device and could be very promising for clinical applications.

## Supplementary Material

Refer to Web version on PubMed Central for supplementary material.

## Acknowledgments

The authors are grateful for the funding of this research, which was made possible in part through the National Institute of General Medical Sciences (1R01 GM086895), the National Science Foundation (CAREER, CBET-0954360), and the University of Akron (Firestone Fellowship).

## REFERENCES

1. Pepys MB, Hirschfield GM, Tennent GA, Gallimore JR, Kahan MC, Bellotti V, Hawkins PN, Myers RM, Smith MD, Polara A, Cobb AJ, Ley SV, Aquilina JA, Robinson CV, Sharif I, Gray GA, Sabin CA, Jenvey MC, Kolstoe SE, Thompson D, Wood SP. Targeting C-reactive protein for the treatment of cardiovascular disease. Nature. 2006; 440(7088):1217–1221. [PubMed: 16642000]
2. Koning GA, Schiffelers RM, Wauben MH, Kok RJ, Mastrobattista E, Molema G, ten Hagen TL, Storm G. Targeting of angiogenic endothelial cells at sites of inflammation by dexamethasone phosphate-containing RGD peptide liposomes inhibits experimental arthritis. Arthritis Rheum. 2006; 54(4):1198–1208. [PubMed: 16575845]
3. Bakker-Woudenberg IA, Lokerse AF, ten Kate MT, Mouton JW, Woodle MC, Storm G. Liposomes with prolonged blood circulation and selective localization in Klebsiella pneumoniae-infected lung tissue. J Infect Dis. 1993; 168(1):164–171. [PubMed: 8515105]
4. Kukowska-Latallo JF, Candido KA, Cao Z, Nigavekar SS, Majoros IJ, Thomas TP, Balogh LP, Khan MK, Baker JR Jr. Nanoparticle targeting of anticancer drug improves therapeutic response in animal model of human epithelial cancer. Cancer Res. 2005; 65(12):5317–5324. [PubMed: 15958579]
5. Goldsmith MA, Slavik M, Carter SK. Quantitative prediction of drug toxicity in humans from toxicology in small and large animals. Cancer Res. 1975; 35(5):1354–1364. [PubMed: 804350]
6. Harrington EA, Bebbington D, Moore J, Rasmussen RK, Ajose-Adeogun AO, Nakayama T, Graham JA, Demur C, Hercend T, Diu-Hercend A, Su M, Golec JM, Miller KM. VX-680, a potent and selective small-molecule inhibitor of the Aurora kinases, suppresses tumor growth in vivo. Nat Med. 2004; 10(3):262–267. [PubMed: 14981513]
7. Saga T, Neumann RD, Heya T, Sato J, Kinuya S, Le N, Paik CH, Weinstein JN. Targeting cancer micrometastases with monoclonal antibodies: a binding-site barrier. Proc Natl Acad Sci U S A. 1995; 92(19):8999–9003. [PubMed: 7568060]
8. Barry MA, Dower WJ, Johnston SA. Toward cell-targeting gene therapy vectors: selection of cell-binding peptides from random peptide-presenting phage libraries. Nat Med. 1996; 2(3):299–305. [PubMed: 8612228]
9. Dreher MR, Liu W, Michelich CR, Dewhirst MW, Yuan F, Chilkoti A. Tumor vascular permeability, accumulation, and penetration of macromolecular drug carriers. J Natl Cancer Inst. 2006; 98(5):335–344. [PubMed: 16507830]
10. Kirpotin DB, Drummond DC, Shao Y, Shalaby MR, Hong K, Nielsen UB, Marks JD, Benz CC, Park JW. Antibody targeting of long-circulating lipidic nanoparticles does not increase tumor localization but does increase internalization in animal models. Cancer Res. 2006; 66(13):6732–6740. [PubMed: 16818648]
11. Bagnato JD, Eilers AL, Horton RA, Grissom CB. Synthesis and characterization of a cobalamin-colchicine conjugate as a novel tumor-targeted cytotoxin. J Org Chem. 2004; 69(26):8987–8996. [PubMed: 15609930]



$watermark-text
$watermark-text
$watermark-text

$watermark-text

$watermark-text

$watermark-text


12. Stangelberger A, Schally AV, Letsch M, Szepeshazi K, Nagy A, Halmos G, Kanashiro CA, Corey E, Vessella R. Targeted chemotherapy with cytotoxic bombesin analogue AN-215 inhibits growth of experimental human prostate cancers. Int J Cancer. 2006; 118(1):222–229. [PubMed: 16003723]
13. Patrick TA, Kranz DM, van Dyke TA, Roy EJ. Folate receptors as potential therapeutic targets in choroid plexus tumors of SV40 transgenic mice. J Neurooncol. 1997; 32(2):111–123. [PubMed: 9120540]
14. Nakashima-Matsushita N, Homma T, Yu S, Matsuda T, Sunahara N, Nakamura T, Tsukano M, Ratnam M, Matsuyama T. Selective expression of folate receptor beta and its possible role in methotrexate transport in synovial macrophages from patients with rheumatoid arthritis. Arthritis Rheum. 1999; 42(8):1609–1616. [PubMed: 10446858]
15. Garin-Chesa P, Campbell I, Saigo PE, Lewis JL Jr, Old LJ, Rettig WJ. Trophoblast and ovarian cancer antigen LK26. Sensitivity and specificity in immunopathology and molecular identification as a folate-binding protein. Am J Pathol. 1993; 142(2):557–567. [PubMed: 8434649]
16. Parker N, Turk MJ, Westrick E, Lewis JD, Low PS, Leamon CP. Folate receptor expression in carcinomas and normal tissues determined by a quantitative radioligand binding assay. Anal Biochem. 2005; 338(2):284–293. [PubMed: 15745749]
17. Antony AC. Folate receptors. Annu Rev Nutr. 1996; 16:501–521. [PubMed: 8839936]
18. Sun XL, Murphy BR, Li QJ, Gullapalli S, Mackins J, Jayaram HN, Srivastava A, Antony AC. Transduction of folate receptor cDNA into cervical carcinoma cells using recombinant adeno-associated virions delays cell proliferation in vitro and in vivo. J Clin Invest. 1995; 96(3):1535–1547. [PubMed: 7657824]
19. Kelemen LE. The role of folate receptor alpha in cancer development, progression and treatment: cause, consequence or innocent bystander? Int J Cancer. 2006; 119(2):243–250. [PubMed: 16453285]
20. Paulos CM, Reddy JA, Leamon CP, Turk MJ, Low PS. Ligand binding and kinetics of folate receptor recycling in vivo: impact on receptor-mediated drug delivery. Mol Pharmacol. 2004; 66(6):1406–1414. [PubMed: 15371560]
21. Leamon CP, Pastan I, Low PS. Cytotoxicity of folate-Pseudomonas exotoxin conjugates toward tumor cells. Contribution of translocation domain. J Biol Chem. 1993; 268(33):24847–24854. [PubMed: 8227046]
22. Ditto AJ, Shah PN, Lopina ST, Yun YH. Nanospheres formulated from L-tyrosine polyphosphate as a potential intracellular delivery device. Int J Pharm. 2009; 368(1–2):199–206. [PubMed: 19026734]
23. Gupta AS, Lopina ST. Properties of L-tyrosine based polyphosphates pertinent to biomedical applications. Polymer. 2005; 46:2133–2140.
24. Hindi KM, Ditto AJ, Panzner MJ, Medvetz DA, Han DS, Hovis CE, Hilliard JK, Taylor JB, Yun YH, Cannon CL, Youngs WJ. The antimicrobial efficacy of sustained release silver-carbene complex-loaded L-tyrosine polyphosphate nanoparticles: characterization, in vitro and in vivo studies. Biomaterials. 2009; 30(22):3771–3779. [PubMed: 19395021]
25. Ditto AJ, Shah PN, Gump LR, Yun YH. Nanospheres formulated from L-tyrosine polyphosphate exhibiting sustained release of polyplexes and in vitro controlled transfection properties. Mol Pharm. 2009; 6(3):986–995. [PubMed: 19341289]
26. Liong M, Lu J, Kovochich M, Xia T, Ruehm SG, Nel AE, Tamanoi F, Zink JI. Multifunctional inorganic nanoparticles for imaging, targeting, and drug delivery. ACS Nano. 2008; 2(5):889–896. [PubMed: 19206485]
27. Stella B, Arpicco S, Peracchia MT, Desmaele D, Hoebeke J, Renoir M, D'Angelo J, Cattel L, Couvreur P. Design of folic acid-conjugated nanoparticles for drug targeting. J Pharm Sci. 2000; 89(11):1452–1464. [PubMed: 11015690]
28. Kohler N, Sun C, Fichtenholtz A, Gunn J, Fang C, Zhang M. Methotrexate-immobilized poly(ethylene glycol) magnetic nanoparticles for MR imaging and drug delivery. Small. 2006; 2(6):785–792. [PubMed: 17193123]

$watermark-text

$watermark-text

$watermark-text


29. Sun C, Sze R, Zhang M. Folic acid-PEG conjugated superparamagnetic nanoparticles for targeted cellular uptake and detection by MRI. J Biomed Mater Res A. 2006; 78(3):550–557. [PubMed: 16736484]
30. Matsumoto T, Kajiya F. Coronary microcirculation: Physiology and mechanics. Fluid Dynamic Res. 2005; 37:60–61.
31. Shi ZD, Ji XY, Qazi H, Tarbell JM. Interstitial flow promotes vascular fibroblast, myofibroblast, and smooth muscle cell motility in 3-D collagen I via upregulation of MMP-1. Am J Physiol Heart Circ Physiol. 2009; 297(4):H1225–H1234. [PubMed: 19465549]
32. Rothberg KG, Ying YS, Kolhouse JF, Kamen BA, Anderson RG. The glycophospholipid-linked folate receptor internalizes folate without entering the clathrin-coated pit endocytic pathway. J Cell Biol. 1990; 110(3):637–649. [PubMed: 1968465]
33. Yoo HS, Park TG. Folate receptor targeted biodegradable polymeric doxorubicin micelles. J Control Release. 2004; 96(2):273–283. [PubMed: 15081218]
34. Medvetz DA, Hindi KM, Panzner MJ, Ditto AJ, Yun YH, Youngs WJ. Anticancer Activity of Ag(I) N-Heterocyclic Carbene Complexes Derived from 4,5-Dichloro-1H-Imidazole. Met Based Drugs. 2008; 2008 384010.
35. Patil VR, Campbell CJ, Yun YH, Slack SM, Goetz DJ. Particle diameter influences adhesion under flow. Biophys J. 2001; 80(4):1733–1743. [PubMed: 11259287]
36. Yun YH, Goetz DJ, Yellen P, Chen W. Hyaluronan microspheres for sustained gene delivery and site-specific targeting. Biomaterials. 2004; 25(1):147–157. [PubMed: 14580918]
37. Brown DC, Larson RS. Improvements to parallel plate flow chambers to reduce reagent and cellular requirements. BMC Immunol. 2001; 2:9. [PubMed: 11580861]
38. Mathias CJ, Lewis MR, Reichert DE, Laforest R, Sharp TL, Lewis JS, Yang ZF, Waters DJ, Snyder PW, Low PS, Welch MJ, Green MA. Preparation of 66Ga- and 68Ga-labeled Ga(III)-deferoxamine-folate as potential folate-receptor-targeted PET radiopharmaceuticals. Nucl Med Biol. 2003; 30(7):725–731. [PubMed: 14499330]
39. Ditto AJ, Shah PN, Yun YH. Non-viral gene delivery using nanoparticles. Expert Opin Drug Deliv. 2009
40. Leid JG, Ditto AJ, Knapp A, Shah PN, Wright BD, Blust R, Christensen L, Clemons CB, Wilber JP, Young GW, Kang AG, Panzner MJ, Cannon CL, Yun YH, Youngs WJ, Seckinger NM, Cope EK. In vitro antimicrobial studies of silver carbene complexes: activity of free and nanoparticle carbene formulations against clinical isolates of pathogenic bacteria. J Antimicrob Chemother. 2012; 67(1):138–148. [PubMed: 21972270]
41. Friedrich CL, Moyles D, Beveridge TJ, Hancock RE. Antibacterial action of structurally diverse cationic peptides on gram-positive bacteria. Antimicrob Agents Chemother. 2000; 44(8):2086–2092. [PubMed: 10898680]
42. Ross JF, Chaudhuri PK, Ratnam M. Differential regulation of folate receptor isoforms in normal and malignant tissues in vivo and in established cell lines. Physiologic and clinical implications. Cancer. 1994; 73(9):2432–2443. [PubMed: 7513252]
43. Kruman II, Kumaravel TS, Lohani A, Pedersen WA, Cutler RG, Kruman Y, Haughey N, Lee J, Evans M, Mattson MP. Folic acid deficiency and homocysteine impair DNA repair in hippocampal neurons and sensitize them to amyloid toxicity in experimental models of Alzheimer's disease. J Neurosci. 2002; 22(5):1752–1762. [PubMed: 11880504]
44. Desai MP, Labhasetwar V, Walter E, Levy RJ, Amidon GL. The mechanism of uptake of biodegradable microparticles in Caco-2 cells is size dependent. Pharm Res. 1997; 14(11):1568–1573. [PubMed: 9434276]
45. Foged C, Brodin B, Frokjaer S, Sundblad A. Particle size and surface charge affect particle uptake by human dendritic cells in an in vitro model. Int J Pharm. 2005; 298(2):315–322. [PubMed: 15961266]
46. Astier A, Doat B, Ferrer MJ, Benoit G, Fleury J, Rolland A, Leverge R. Enhancement of adriamycin antitumor activity by its binding with an intracellular sustained-release form, polymethacrylate nanospheres, in U-937 cells. Cancer Res. 1988; 48(7):1835–1841. [PubMed: 2894892]

$watermark-text

$watermark-text

$watermark-text


47. Akinc A, Thomas M, Klibanov AM, Langer R. Exploring polyethylenimine-mediated DNA transfection and the proton sponge hypothesis. J Gene Med. 2005; 7(5):657–663. [PubMed: 15543529]
48. Maeda H, Sawa T, Konno T. Mechanism of tumor-targeted delivery of macromolecular drugs, including the EPR effect in solid tumor and clinical overview of the prototype polymeric drug SMANCS. J Control Release. 2001; 74(1–3):47–61. [PubMed: 11489482]
49. Cozens-Roberts C, Quinn JA, Lauffenberger DA. Receptor-mediated adhesion phenomena. Model studies with the Radical-Flow Detachment Assay. Biophys J. 1990; 58(1):107–125. [PubMed: 2166596]
50. Muro S, Dziubla T, Qiu W, Leferovich J, Cui X, Berk E, Muzykantov VR. Endothelial targeting of high-affinity multivalent polymer nanocarriers directed to intercellular adhesion molecule 1. J Pharmacol Exp Ther. 2006; 317(3):1161–1169. [PubMed: 16505161]
51. Leamon CP, Low PS. Delivery of macromolecules into living cells: a method that exploits folate receptor endocytosis. Proc Natl Acad Sci U S A. 1991; 88(13):5572–5576. [PubMed: 2062838]
52. Dickerson JB, Blackwell JE, Ou JJ, Patil VR, Goetz DJ. Limited adhesion of biodegradable microspheres to E- and P-selectin under flow. Biotechnol Bioeng. 2001; 73(6):500–509. [PubMed: 11344455]
53. Malek AM, Alper SL, Izumo S. Hemodynamic shear stress and its role in atherosclerosis. Jama. 1999; 282(21):2035–2042. [PubMed: 10591386]
54. Pujol Cubells M, Prat Aixela J, Girona Brumos V, Duran Pou S, Villaronga Flaque M. Stability of cisplatin in sodium chloride 0.9% intravenous solution related to the container's material. Pharm World Sci. 1993; 15(1):34–36. [PubMed: 8485505]
55. Wong HL, Bendayan R, Rauth AM, Xue HY, Babakhanian K, Wu XY. A mechanistic study of enhanced doxorubicin uptake and retention in multidrug resistant breast cancer cells using a polymer-lipid hybrid nanoparticle system. J Pharmacol Exp Ther. 2006; 317(3):1372–1381. [PubMed: 16547167]
56. Na K, Bum Lee T, Park KH, Shin EK, Lee YB, Choi HK. Self-assembled nanoparticles of hydrophobically-modified polysaccharide bearing vitamin H as a targeted anti-cancer drug delivery system. Eur J Pharm Sci. 2003; 18(2):165–173. [PubMed: 12594010]
57. Yeo EJ, Chun YS, Cho YS, Kim J, Lee JC, Kim MS, Park JW. YC-1: a potential anticancer drug targeting hypoxia-inducible factor 1. J Natl Cancer Inst. 2003; 95(7):516–525. [PubMed: 12671019]
58. Lee RJ, Low PS. Delivery of liposomes into cultured KB cells via folate receptor-mediated endocytosis. J Biol Chem. 1994; 269(5):3198–3204. [PubMed: 8106354]
59. Lokich J, Anderson N. Carboplatin versus cisplatin in solid tumors: an analysis of the literature. Ann Oncol. 1998; 9(1):13–21. [PubMed: 9541678]
60. Ardizzoni A, Boni L, Tiseo M, Fossella FV, Schiller JH, Paesmans M, Radosavljevic D, Paccagnella A, Zatloukal P, Mazzanti P, Bisse D, Rosell R. Cisplatin- Versus Carboplatin-Based Chemotherapy in First-Line Treatment of Advanced Non-Small-Cell Lung Cancer: An Individual Patient Data Meta-analysis. J Natl Cancer Inst. 2007; 99(11):847–857. [PubMed: 17551145]

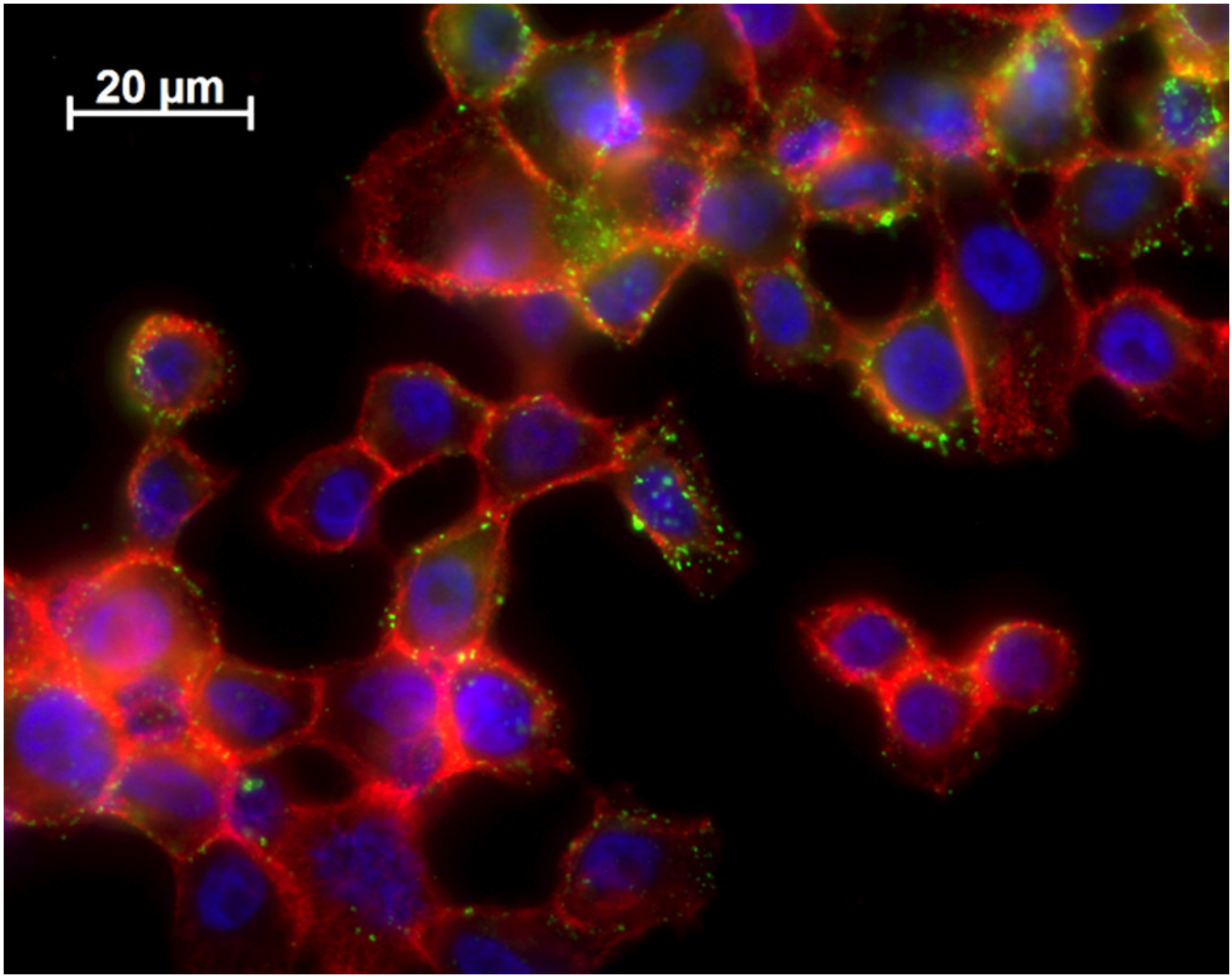


$watermark-text
$watermark-text
$watermark-text

$watermark-text

$watermark-text

$watermark-text

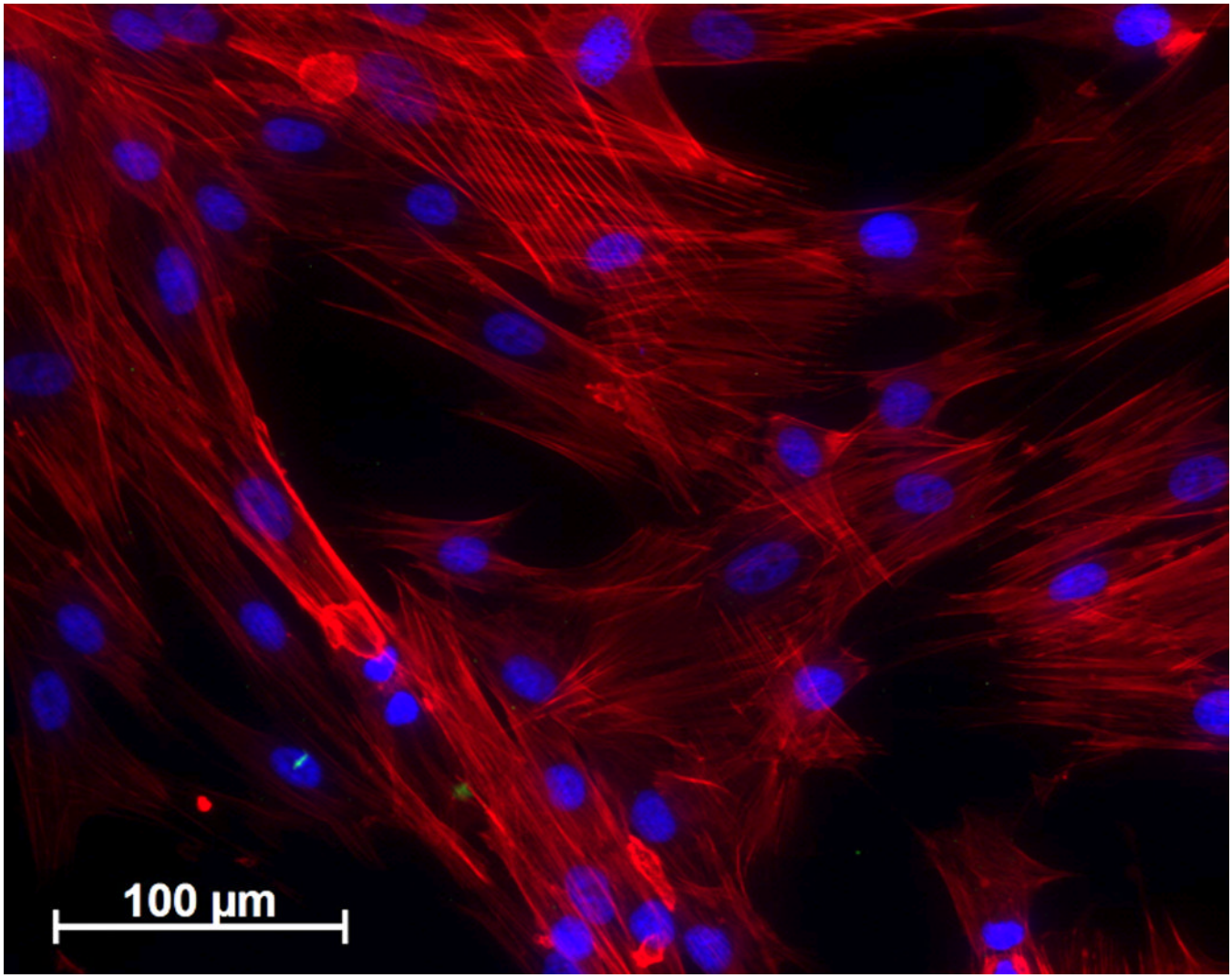


**Figure 1.**
Microscopy of FR-α for A) HeLa and B) fibroblasts. Folate receptor was detected with primary antibody using anti-FR-α mouse IgG and secondary antibody of anti-mouse IgG conjugated to FITC (green). In addition, Hoechst stained was used to detect the nuclei (blue) and rhodamine phalloidin stained the cells's cytoskeleton (red).

$watermark-text
$watermark-text
$watermark-text

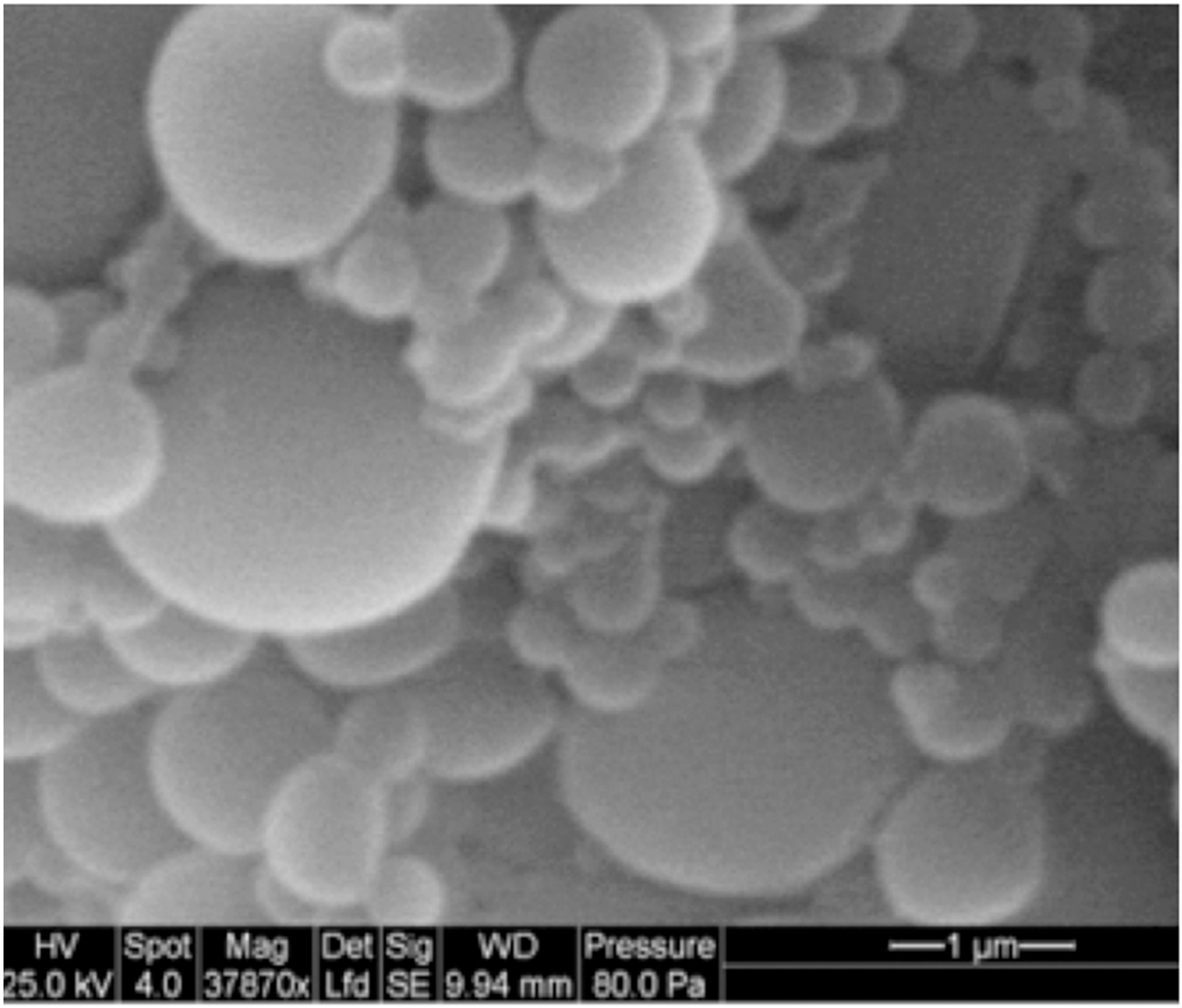


**Figure 2.**
Scanning electron microscopy (40,000×) of targeted nanoparticles.

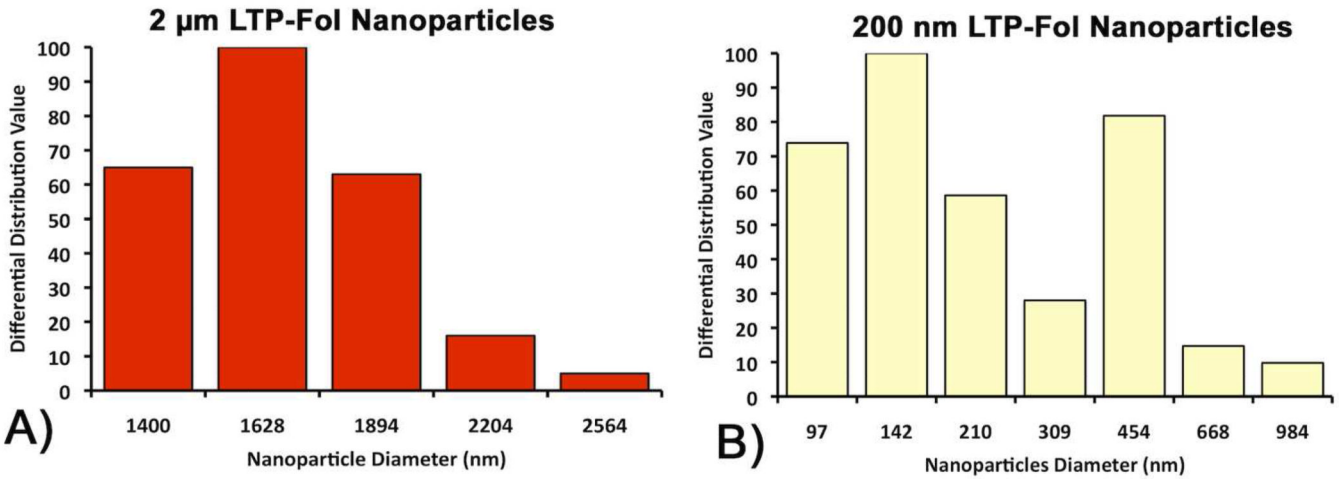


**Figure 3.**
Dynamic Light Scattering. Size distributions of A) 2 µm targeted nanoparticles and B) 200 nm targeted nanoparticles.

$watermark-text
$watermark-text
$watermark-text

$watermark-text
$watermark-text
$watermark-text

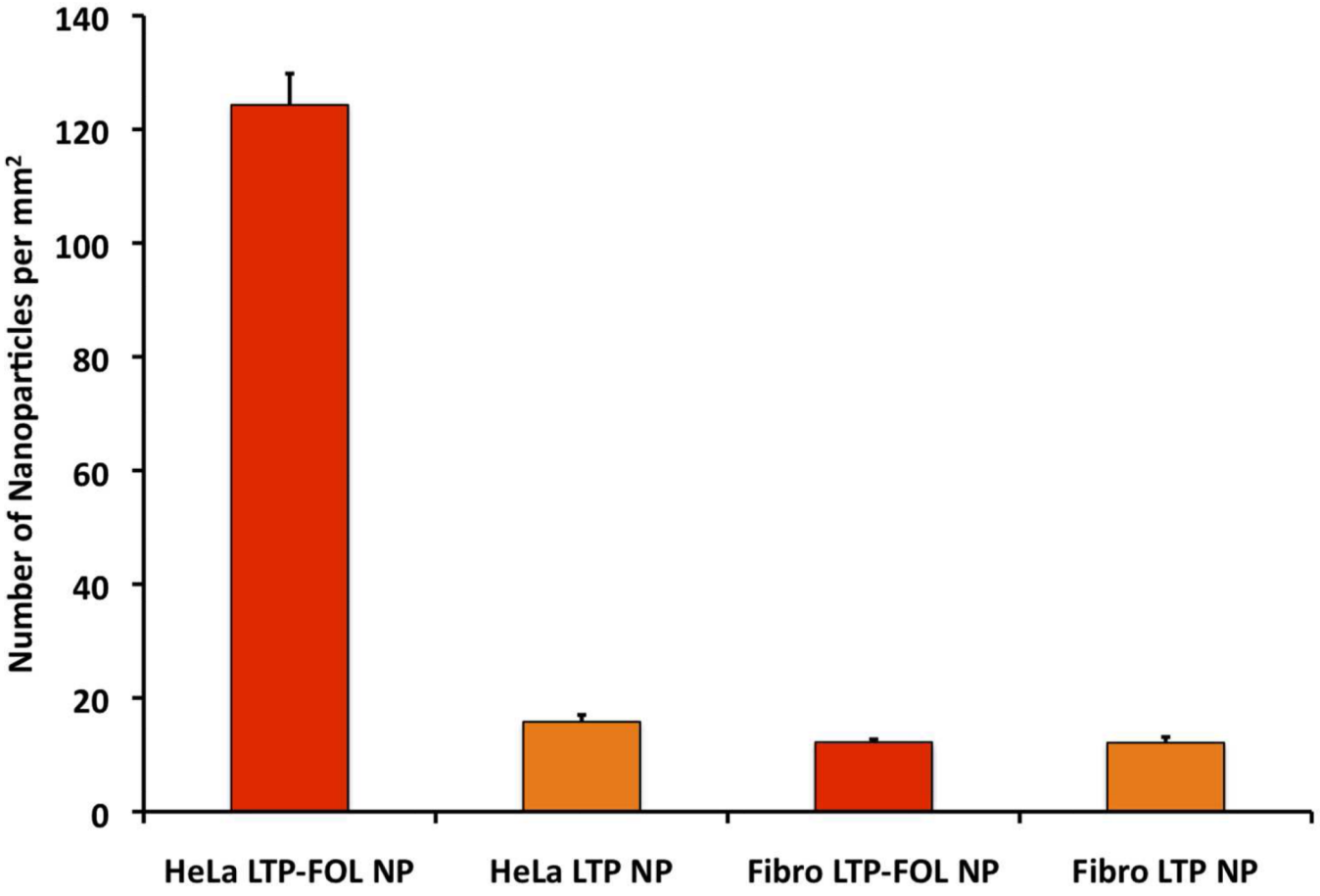


**Figure 4.**
Nanoparticle attachment. Number of attached targeted and plain nanoparticles per square millimeter on both HeLa and primary human dermal fibroblasts.

$watermark-text
$watermark-text
$watermark-text

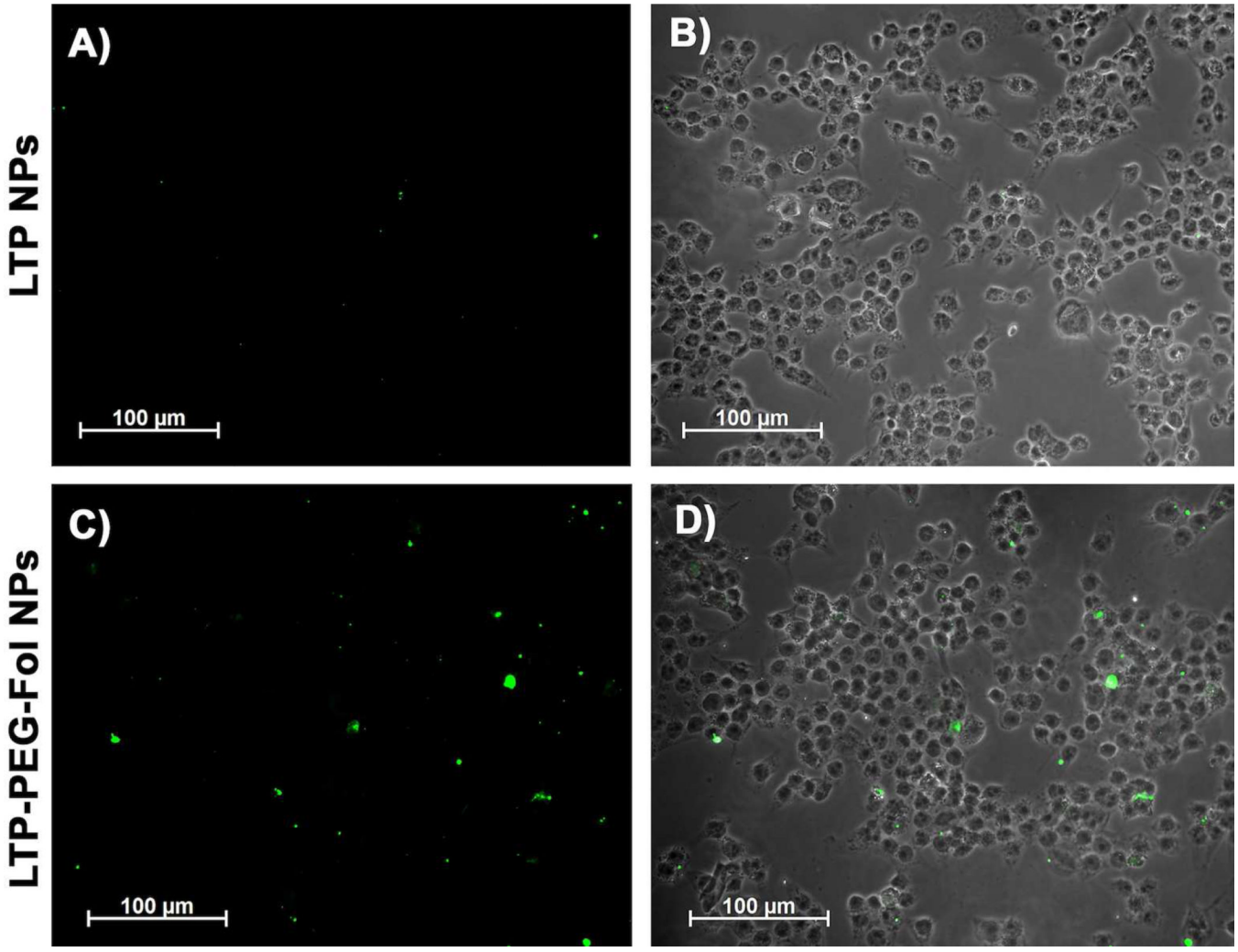


**Figure 5.**
Attachment of nanoparticles labeled with FITC. Plain (A–B) and targeted (C–D) nanoparticles loaded with FITC attachment to HeLa under simulated physiological flow at 0.5 dynes/cm$^2$. (A) FITC channel and (B) combined FITC and phase contrast image. (C) FITC channel and (D) combined FITC and phase contrast image for targeted nanoparticles.

$watermark-text
$watermark-text
$watermark-text

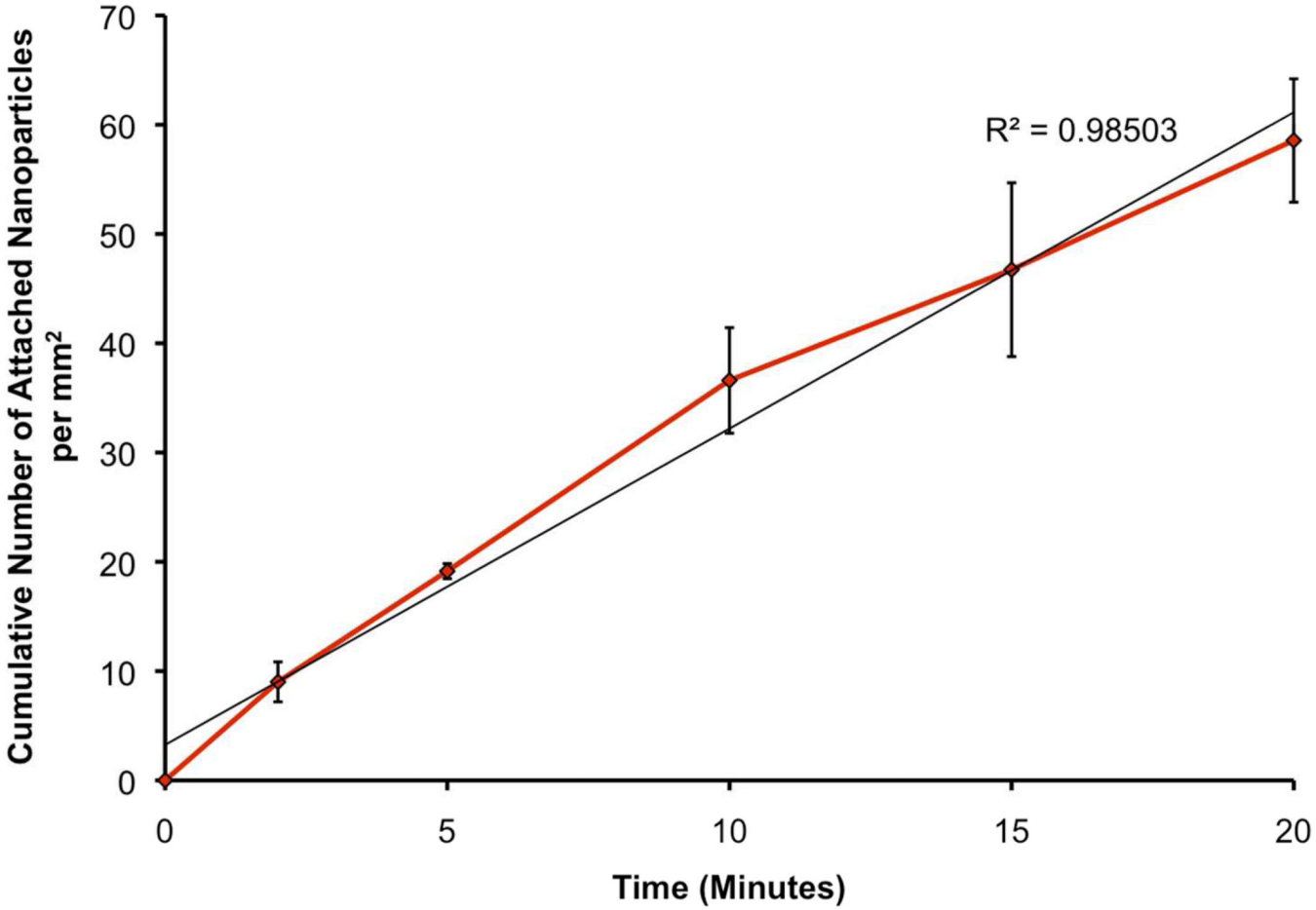


**Figure 6.**
Attachment kinetics. Number of targeted nanoparticles attached to HeLa under shear stress of 0.5 dynes/cm$^2$ as a function of time.

$watermark-text

$watermark-text

$watermark-text

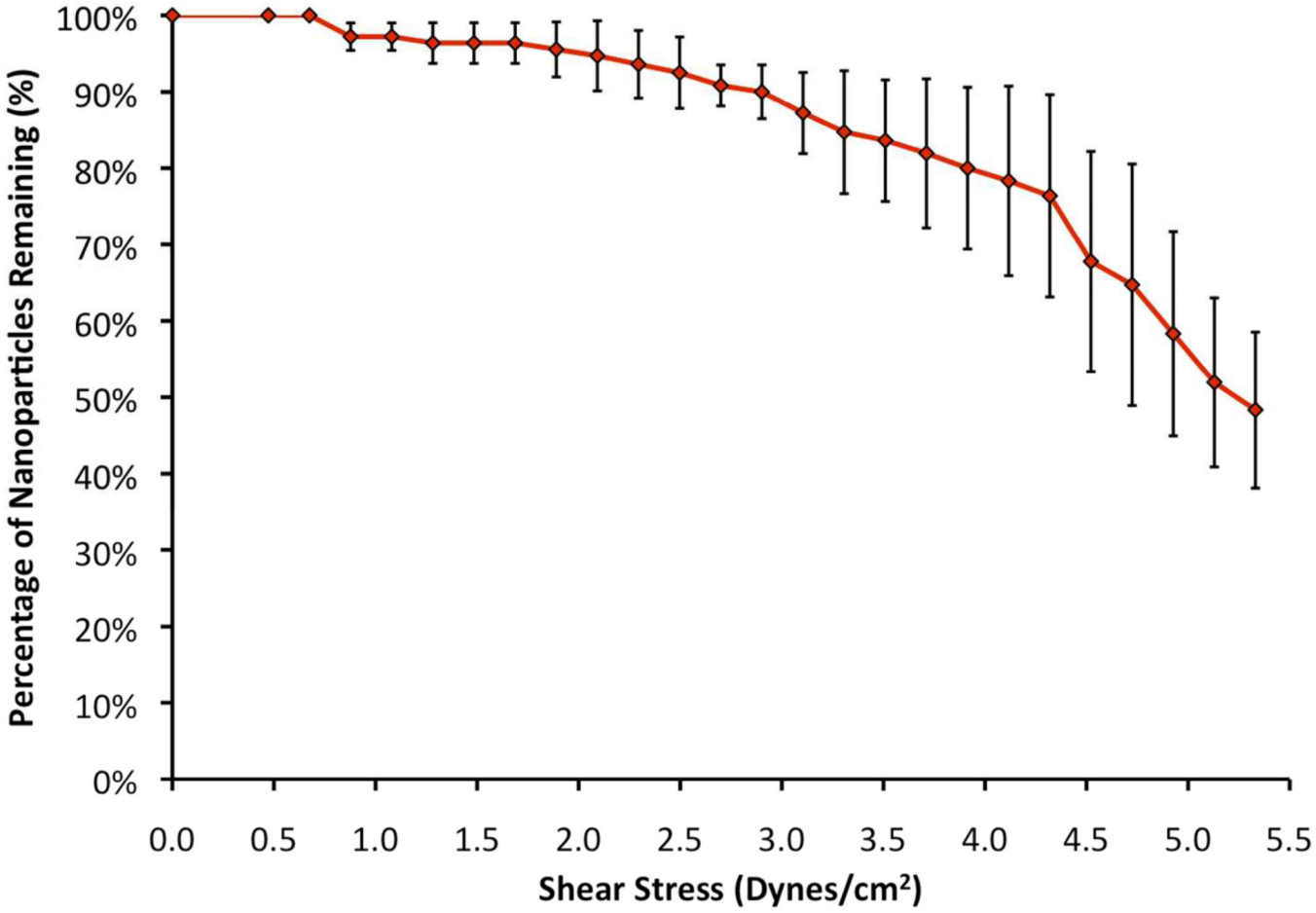


**Figure 7.**
The strength of the nanoparticle attachment. The percentage of targeted nanoparticles remaining attached to HeLa with increasing shear stresses.

$watermark-text
$watermark-text
$watermark-text

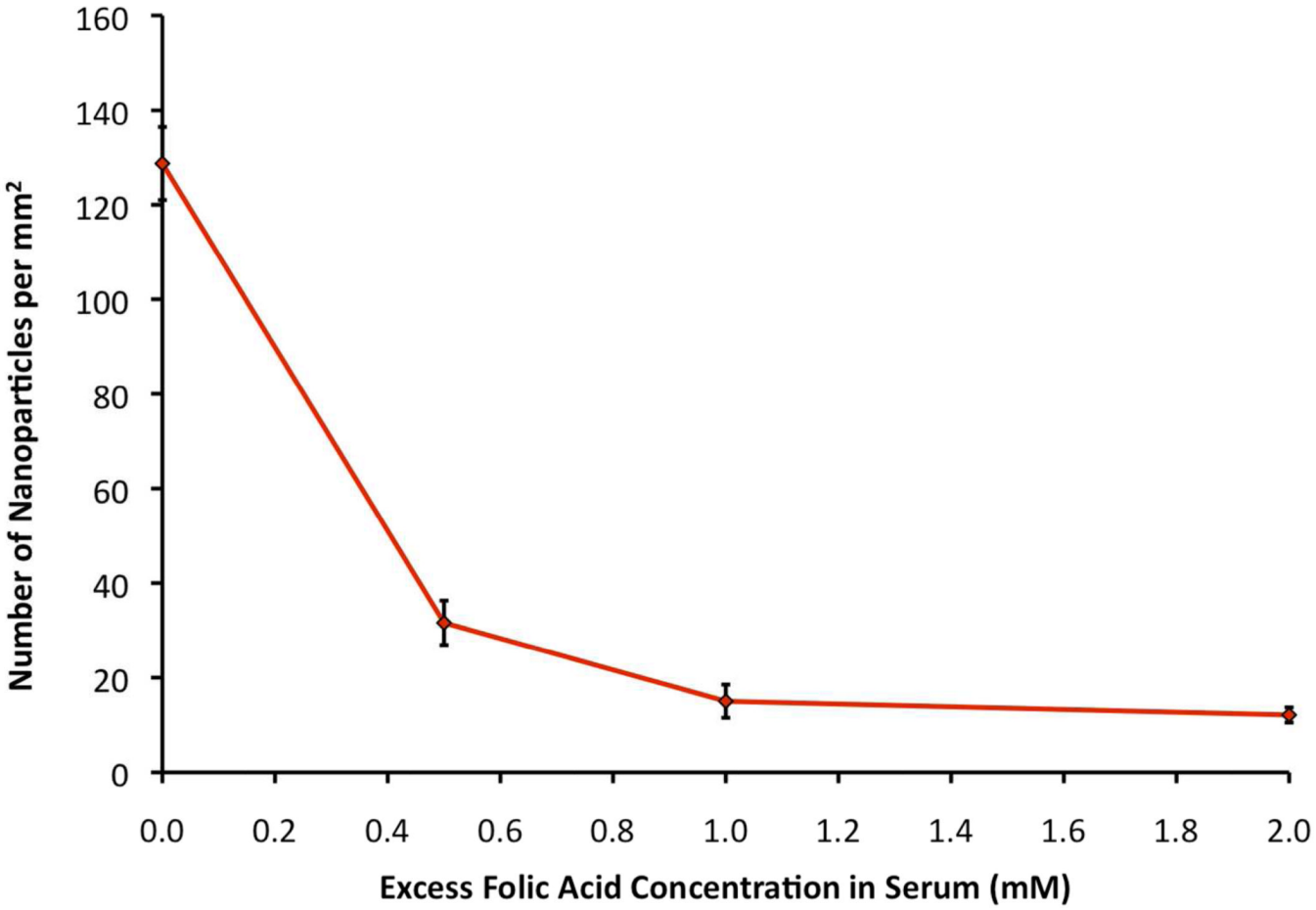


**Figure 8.**
Inhibition of targeted nanoparticle attachment. A competition assay was performed by adding excess folic acid to the perfusion medium. As expected, number of nanoparticle decreased due to presence of folic acid.

$watermark-text

$watermark-text

$watermark-text

## Table 1

Anticancer activity of drug loaded targeted nanoparticles, drug loaded plain nanoparticles, and anticancer drugs.

| | HeLa Viability | FibroblastsViability |
|---|---|---|
| Untreated Cells | 92 ± 1% | 95 ± 2% |
| Blank LTP-Fol Nanoparticles | 93 ± 2% | 97 ± 1% |
| SCC22 * | 93 ± 2% | 92 ± 3% |
| SCC22-LTP Nanoparticles * | 93 ± 1% | 92 ± 3% |
| **SCC22-LTP-Fol Nanoparticles** * | **54 ± 5%** | **93 ± 2%** |
| Cisplatin † | 103 ± 6% | 101 ± 13 % |
| Cisplatin-LTP Nanoparticles † | 64± 7% | 73 ± 14 % |
| **Cisplatin-LTP-Fol Nanoparticles** † | **53 ± 6%** | **64 ± 6%** |

The drug concentrations within the nanoparticles is 12 μM* for SCC22 and 0.63 μM† for cisplatin